UNIVERSITY OF CALIFORNIA SAN DIEGO

P209L Mutation in BAG3 Does Not Cause Cardiomyopathy in Mice

A Thesis submitted in partial satisfaction of the requirements for the degree
Master of Science

in

Biology

by

Paul Zhou

Committee in charge:

Ju Chen, Chair
Michael David, Co-Chair
Jon Christopher Armour

2018

The Thesis of Paul Zhou is approved, and it is acceptable in quality and form for publication on microfilm and electronically:

Co-Chair

Chair

University of California San Diego

2018

DEDICATION

I dedicate this thesis to my incredible parents, who gave meaning to my life. Without their immense sacrifice and unconditional love, I would never be able to achieve my dream.

TABLE OF CONTENTS

LIST OF ABBREVIATIONS

sHsps: Small heat shock proteins

HSP70: Heat Shock Protein 70

PQC: protein quality control system

NBD: nucleotide-binding domain

BAG3: Bcl-associated athanogene 3

HSPB: ATP-independent small heat shock proteins

HSPB5 (αB-crystallin): small Heat Shock Protein Family B Member 5

HSPB6 (Hsp20): small Heat Shock Protein Family B Member 6

HSPB7: small Heat Shock Protein Family B (Small) Member 7

HSPB8 (Hsp22): small Heat Shock Protein Family B (Small) Member 8

GWAS: genome-wide association study

E455K: A single amino acid substitution of glutamic acid 455 to lysine (E455K) in BAG domain of BAG3

DCM: dilated cardiomyopathy

CKO: Cardiomyocyte specific knockout

IPV: Ile-Pro-Val (IPV) motif in BAG3, responsible for binding sHSPs

P209L: a single amino acid substitution of Proline 209 to Leucine in the IPV motif of BAG3

αMHC: mouse cardiac-specific alpha-myosin heavy chain promoter

ATP: Adenosine Tri-Phosphate

HSC70: Heat shock cognate protein 70

GPG: amino acid Glycine-Proline-Glycine

WW domain: composed of 40 amino acids with two conserved Tryptophans

PxxP region: Src homology region 3 (SH3) ligand region

LIST OF FIGURES

ACKNOWLEDGEMENTS

I would like to acknowledge Ju Chen for the privilege to be part of his research team. The Chen Lab has not only been an essential part of my academic experience but also a place for my personal growth here at UC San Diego. Ju has devoted himself wholeheartedly to empower all members of the lab, regardless of what our ultimate career goals might be. Through his tireless effort, the Chen lab has been a big family with diverse talents, in which everyone is able to flourish. I benefited greatly from this nurturing environment, and it would not have been possible without the mentorship, friendship, and generous support of Ju, postdoctoral scholars, graduate students, and other members of the lab.

My genuine appreciation also goes to Michael David and Chris Armour for the time and effort they invested to be on my committee. Moreover, I would like to thank them for being exceptional educators and mentors who are truly dedicated to the learning community at UC San Diego. I am grateful for the privilege to learn from and interact with students under their instruction. Their influence has not only imparted upon me the importance of teaching and mentoring students but also enabled me to experience the rewards firsthand.

In conclusion, I would like to thank Xi Fang, Xiaolong Ma, Julius Bogomolvous, Wei Feng, Canzhao Liu, and Yongxin Mu for everything they have taught me about molecular cardiology research and beyond. Through their guidance and genius, I learned what true scientific inquiry is about and have been able to acquire the rigorous discipline and commitment needed for research. I can only imagine the patience and love they have invested in me, which I am forever grateful.

ABSTRACT OF THE THESIS

P209L Mutation in BAG3 Does Not Cause Cardiomyopathy in Mice
by

Paul Zhou

Master of Science in Biology

University of California San Diego, 2018

Professor Ju Chen, Chair

Professor Michael David, Co-Chair

Cardiomyocytes are under constant mechanical and metabolic stress, which makes functional protein quality control (PQC) systems particularly important. Molecular chaperones and co-chaperones are essential components of a functioning PQC. Mutation and downregulation of the co-chaperone protein BCL-2–associated athanogene 3 (BAG3) are associated with cardiomyopathy and heart failure. It has been reported that a BAG3 P209L missense mutation leads to the development of myofibrillar myopathy with severe cardiac defects. However, the mechanisms by which the P209L mutation leads to cardiomyopathy remain obscure. In our present study, we found that BAG3 P209L mutation in mouse did not cause cardiomyopathy. In the molecular level, the levels of

ATP-dependent and ATP-independent heat shock proteins were not changed in cardiac tissues from BAG3 P209L mutant mice. Further experiments revealed that the P209L mutation did not influence the levels of autophagy or global ubiquitination in cardiac tissues. Together, these observations suggest that the BAG3 209L mutation alone may not cause cardiomyopathy in mice.

INTRODUCTION

Protein quality control and molecular chaperone in cardiomyocyte:

Cardiomyocytes are constantly faced with the challenge to efficiently and properly fold nascent polypeptides, traffic them to their appropriate cellular locations, and prevent them from denaturing when exposed to physiological and pathological stimuli (1). Cardiomyocytes have developed a multilayer protein quality control (PQC) system to maintain protein homeostasis and cardiac function (1). Central players of the cellular PQC system are molecular chaperones and co-chaperones that function to stabilize correct protein conformations, refold aberrant proteins to their functionally active native state, or target unfolded, misfolded or aggregated substrates for degradation (2-4).

Molecular chaperones are proteins that assist in folding or unfolding of individual proteins, and the assembly or disassembly of macromolecular structures. Multiple specialized proteins form a complex chaperone network that mediates the correct folding of nascent or aberrant peptides to prevent misfolding and the subsequent formation of aggregates. There are two general categories of molecular chaperones, the first of which is the ATP-dependent high-molecular-weight HSPs such as the HSP70 family. HSP70 uses the energy from ATP hydrolysis to regulate reversible binding to unfolded or partially folded proteins to ultimately refold these proteins into their native conformation. The second category is the ATP-independent small HSP (sHSP/ HSPB) family, for example, HSPB5 (αB-crystallin) HSPB6 (Hsp20), HSPB7, HSPB8 (Hsp22). In the chaperone network, sHSPs function as “holdases”, a term that refers to their ability to bind and stabilize denatured or non-native proteins against aggregation, subsequently bring them to be refolded by HSP70s (55). Co-chaperones, such as BAG3, and are proteins that assist chaperones in protein folding and other functions.

The protein domains and function of co-chaperone protein BAG3:

BAG3 belongs to the BAG family of co-chaperones which includes BAG1-5, characterized by a conserved BAG domain (53). BAG3 is a 61-kDa stress-inducible protein with multiple protein-protein interaction motifs or domains (Figure. 1A). The BAG domain of BAG3 binds to nucleotide binding domain (NBD), which is responsible for ATPase activity, of the ATP-dependent chaperone HSP70 family. HSP70 is heat shock protein that plays a crucial role in folding nascent proteins and assembly and disassembly of other protein structures. BAG3 is a potent nucleotide exchange factor and modulates chaperone protein activities (12, 13). The protein-protein interaction between the BAG domain of BAG3 and HSP70 aids the release of ADP from HSP70 and facilitates nucleotide cycling (56).

In addition to the conserved carboxyl-terminal BAG domain, BAG3 contains a WW (Trp-Trp) domain at the amino-terminus, and a central proline-rich PxxP region, each of which mediates binding to many different protein partners (14). Recently, two IVP (Ile-Pro-Val) motifs separated by ~100 aa in its N-terminus were identified between the WW domain and the PxxP region that mediate interaction of BAG3 with the small heat shock proteins (sHSP/HSPB) (15,16) (Figure. 1A). These IPV motifs, together with the HSP70-binding BAG domain, allow BAG3 to assemble large multi-chaperone complexes. The multiple protein interaction domains facilitate assembly of large chaperone-co-chaperone complexes to regulate diverse cellular processes such as apoptosis, proliferation, cell adhesion and motility, cytoskeletal organization and protein homeostasis. These multifaceted interactions enable BAG3 to modulate protein folding and stability to effect major processes, thereby allowing cardiomyocytes to adapt to stressful stimuli (12, 14, 17-21). The biological functionality of BAG3 could be largely explained by BAG3's

role as a modular, scaffolding factor that brings together sHSPs and HSP70s. BAG3 has been shown involved in multiple functions, such as apoptosis, cytoskeleton organization, autophagy (18), and essential for allowing cells to adapt to various external stimuli (30).

The cardiac role of BAG3:

BAG3 is prominently expressed in cardiac and skeletal muscle tissue and has been shown to colocalize with α-actinin at Z-disks (22). BAG3 plays an essential role in cardiac tissue, and mechanical stress can induce BAG3 expression. In addition to colocalizing with α-actinin at the Z-disks, BAG3 has been detected in various cellular components including the mitochondrial and cytoplasmic fractions (25). Together these data suggest that BAG3 may play a critical role in quality control of proteins at the Z-disk as well as homeostasis of non-myofibrillar proteins. Multiple mutations in BAG3 have been associated with skeletal and cardiac myopathies, highlighting its importance for striated muscle function (5-10). Importantly, decreased levels of BAG3 have also been described in a family with idiopathic DCM and in unrelated patients with end-stage heart failure (14), suggesting BAG3 is involved in both genetic form and acquired form of dilated cardiomyopathy.

It has been reported that global BAG3 knockout mice exhibit impaired postnatal growth and early lethality at 3-4 weeks (22, 23, 55). Cardiomyocyte-specific knockout of BAG3 (CKO) leads to destabilization of sHSPs, resulting in increased insolubility of BAG3 complex substrates and dilated cardiomyopathy (DCM) (55). The E455K mutation in BAG3, which located in BAG domain of BAG3 has been identified as the unequivocal cause of DCM, disrupted the interaction between BAG3 and HSP70. The homozygous global E455K knock-in mice exhibited impaired

postnatal growth and premature lethality at 4 weeks (55). The cardiac specific E455K mutant mice had cardiac phenotypes comparable to BAG3 cardiac specific knockout mice, with severe cardiac enlargement and decreased systolic function. The identical phenotype between BAG3 knockout and E455K mutation demonstrated that the E455K mutation is a loss of function mutation. Interestingly, the protein levels of sHSPs (HSPB5, HSPB6 and HSPB8) were downregulated in E455K mutant hearts. Notably, the BAG3 E455K mutation affects the interaction between BAG3 and HSP70, but not sHSPs, suggesting the ability of BAG3 to interact with HSP70 was essential to the stability of sHSPs. However, little is known about the underlying mechanism in which BAG3 stabilize sHSPs and the functional consequence of the impaired interaction between sHSPs and BAG3.

The potential function of IPV motif in BAG3:

Two IVP (Ile-Pro-Val) motifs are separated by ~100 aa in the N-terminus of BAG3, between the WW domain and the PxxP region (57) (Figure 1A). It has been reported that two IPV motifs bind to small heat shock proteins such as HSPB8 and HSPB6, and facilitates the formation of elaborate molecular chaperones complex. The IVP domains have been shown to bind small heat shock protein (sHSP) such as HSPB5, 6 and 8. Through domain deletions and point mutations, it has been elucidated that BAG3 uses both of its IPV motifs to interact with sHSPs, including HSP27 (HspB1), αB-crystallin (HSPB5), Hsp22 (HSPB8), and HSP20 (HSPB6). For example, mutation of valine to alanine in the IPV motifs weakened the apparent affinity of BAG3 for sHSPs. Furthermore, mutating IPV to GPG or deletion of individual IPV motifs reduced the stoichiometry of the binding interaction from 2:1 to approximately 1:1, whereas removing of

both IPV motifs through mutating them to GPG completely abolishes binding of sHSPs, suggesting that BAG3 utilize both of its IPV motifs to engage in interaction with sHSPs. It has been identified that the heterozygous p.Pro209Leu (P209L) mutation in humans causes severe muscular dystrophy and cardiomyopathy. The P209L mutation is found at amino acid 209 in the Bag3 Ile-Pro-Val (IPV) motif at amino acids 200 to 213 in BAG3. Patients with the BAG3 P209L mutation have reported progressive limb and axial muscle weakness, and they also experienced the development of cardiomyopathy as well as severe respiratory insufficiency in their teens (58).

Cardiomyocyte-specific (αMHC-) BAG3 P209L transgenic mice have been generated and displayed a slow progression of cardiac complications (59). Through gross comparison of αMHC BAG3 P209L and control wild-type littermate, the αMHC BAG3 P209L heart is visibly enlarged under the hematoxylin and eosin staining. Through studying mouse echocardiography, researchers found that the fractional shortening, which is a reliable indicator of cardiac function, is significantly decreased in the αMHC BAG3 P209L transgenic mice compared to the littermate control. However, little is known about the molecular pathophysiology of how this mutation leads to cardiovascular disease. Notably, this αMHC BAG3 P209L mice is a transgenic model that overexpresses P209L mutant BAG3 protein in cardiomyocytes. Thus, a knock-in mouse model, in which the mutant BAG3 gene is under the control of the endogenous locus, is essential to the understanding of the molecular basis underlying the cardiomyopathy caused by the BAG3 P209L mutant protein.

In this study, I aim to investigate whether P209L mutation in BAG3 leads to dilated cardiomyopathy and the potential mechanism in which P209L mutant BAG3 dysregulates cardiomyocytes homeostasis. I utilized a knock-in mouse model in which the endogenous BAG3 gene has been replaced with mutant BAG3 containing the P215L mutation, which is equivalent to the human P209L mutation. We hypothesize that the P209L mutation disrupts the interaction between BAG3 and small heat shock protein and leads to the degradation of sHSPs, eventually resulting in dysregulation of protein homeostasis and cardiomyopathy.

MATERIALS AND METHODS

Animal protocol and consent

All animals used in this study were maintained by the UCSD animal care personnel at the vivarium of Biomedical Research Facility II. Enrichment was provided to mice kept in standard dark/light cycle conditions. The housing condition met the standard requirements of rodent IACUC guidelines, briefly, one to five individuals per cage. The Institutional Animal Care and Use Committee (IACUC) at the University of California San Diego approved all experimental procedures. UCSD has an Animal Welfare Assurance document (A3033-01) on file with the Office of Laboratory Animal Welfare and is fully accredited by the Association for Assessment and Accreditation of Laboratory Animal Care (AAALAC) International.

Mouse models

C57BL/6 mice (strain code: 027) were purchased from Charles River Laboratories. BAG3 P209L (equivalent to the mouse P215L) knock-in mice have been generated and were available in Dr. Ju Chen laboratory. The knock-in mice were generated by standard techniques using a targeting construct (60). Bag3 m/+ heterozygous mutant mice had been backcrossed onto a C57BL/6 background for at least 10 generations. Bag3 m/+ heterozygous mutant mice were subsequently intercrossed to generate homozygous Bag3 m/m mice (BPL mice). The forward primer 5'-AGGCACAGATGCAGCCAGTTAA and reverse primer 5'-GGTCTTCTGGGCTTGGTGGAA are used for genotyping.

Animal procedures and echocardiography

Mice were anesthetized with 1% isoflurane prior to the echocardiographic study. The echocardiography was performed using a FUJIFILM VisualSonics SonoSite Vevo 2100

ultrasound system with a 32- to 55-MHz linear transducer. We used the percentage of FS as an indicator of systolic cardiac function. Measurements of heart rate (HR), left ventricular end-diastolic dimensions (LVED) and left ventricular end-systolic dimensions (LVESD), LV posterior wall thickness (LVPWd), LVIDs, and LVIDd were determined from the LV M-mode tracing.

Protein isolation and Western blot analysis

Total protein extracts were prepared by suspending ground heart tissue in urea lysis buffer (8 M urea, 2 M thiourea, 3% SDS, 75 mM DTT, 0.03% bromophenol blue, 0.05 M Tris-HCl, pH 6.8) (65). Protein lysates were separated on 4% to 12% SDS-PAGE gels (Life Technologies, Thermo Fisher Scientific) and transferred overnight at 4°C onto PVDF membranes (Bio-Rad). After blocking for 1 hour in TBS containing 0.1% Tween-20 (TBST) and 5% dry milk, the membranes were incubated overnight at 4°C with the indicated primary antibody (See Table 1 for antibody list) in blocking buffer containing 2% dry milk. Blots were washed and incubated with HRP-conjugated secondary antibody generated in rabbit (1:5,000) or mouse (1:2,000) (Dako) for 1 hour at room temperature. Immunoreactive protein bands were visualized using ECL reagent (Thermo Fisher Scientific).

Quantitative RT-PCR

We extracted total RNA from mouse left ventricles using TRIzol reagent (Life Technologies, Thermo Fisher Scientific) according to recommendation provided by the manufacturer. The cDNA was synthesized using MMLV Reverse Transcriptase (Bio-Rad. Primer sequences for

quantitative RT-PCR (qRT-PCR) are complimentary to the respective DNA sequence of the proteins. Primer information are listed in Table 2. RT-PCR reactions were performed using SsoFast EvaGreen Real-Time PCR Master Mix (Bio-Rad) in 96-well, low-profile PCR plates in a Bio-Rad CFX96 Thermocycler.

Histology

Hearts were isolated from age- and sex-matched littermates. Prior to being fixed overnight in 4% paraformaldehyde, mouse hearts were washed in PBS. Hearts were then dehydrated in 70% ethanol. Subsequently, dehydrated hearts were embedded in paraffin and coronally sectioned (10-μm thickness). Sections were stained with Masson's trichrome or Hematoxylin and Eosin and then mounted as a standard preparation for imaging. Finally, a Hamamatsu NanoZoomer2.0HT Slide Scanning System was used to image the prepared heart sections.

Statistical analysis

Data distribution was assumed to be normal. Standard spreadsheet software (Microsoft Excel) were used to analyze prepared data, and all errors bars shown in the figures are s.e.m. Statistical analysis was done using GraphPad Prism v6 (GraphPad Software Inc., La Jolla, CA). The final data also involved ANOVA analysis with multiple sample comparisons, Bonferroni *post hoc* testing was performed to discriminate significance relationships. Two-tailed unpaired tests with alpha-value of 0.05 was utilized for *t*-test analysis.

RESULTS

Generation of P209L knock-in mice mutation

BAG3 P209L (equivalent to the mouse P215L) knock-in mice have been generated and existed in Dr. Ju Chen laboratory. The knock-in mice were generated by standard techniques using a targeting construct (60). Figure 1A shows the binding domains of BAG3, including the two IPV motifs and the BAG domain. The endogenous *Bag3* gene was replaced with a mutant *Bag3* gene containing the P215L mutation, which is equivalent to the human P209L mutation (Figure 1B). Genotyping PCR analysis was performed using primers flanking the neomycin (Neo) -FRT site and the P209L mutant site (Figure 1C). It is important to note that the neomycin gene was removed by crossing with FLP deleter mice after germline-transmission. Based on the method, the genotyping PCR product of mutant allele is 715bp, while the 605bp product is amplified from wild-type allele. As shown in Figure 1B, we detected double bands in the heterozygous P209L mutant, single band at 715 bp in the homozygous P209L mutant, and single band at 605 bp in wild-type control in the PCR result. The Sanger Sequencing results further demonstrate that the endogenous gene was replaced with the Bag3 P209L mutant gene (Figure 1D). Western blot analysis showed that BAG3 protein levels in the hearts of BAG3 heterozygous and homozygous P209L mice lines were comparable to BAG3 protein levels in WT control littermates indicating that the BAG3 P209L mutation does not impair the expression or stability of BAG3 (Figure 1E).

BAG3 P209L mutant mice display normal cardiac structure and function

BAG3 P209L mutant mice are viable and born at expected Mendelian ratios with no observed growth defects. First, we analyze the survival curve of the BAG3 P209L heterozygous (m/+) mice, BAG3 P209L homozygous (m/m) mice along with the control littermates to investigate the effects of the P209L mutation on the overall survival and developmental

progression. We analyzed survival data of the heterozygous and homozygous P209L knock-in mice and control littermates using Kaplan-Meier survival analysis with a log-rank method of statistics (55). The two mutant mouse lines were all viable at birth. No premature death of BAG3 P209L mice is observed; they do not possess increased susceptibility to premature death compared with control littermates (Figure 2A). Over 83% of BAG3 m/+ and m/m mice survived when the last measurement was collected. There was no significant difference among the m/m, m/+, and the control littermates. At Week 66 in adulthood, there was no statistical difference in terms of survival rate among all three mouse lines (Figure 2A).

Next, to examine the overall cardiac phenotype, we measured heart weight, body weight, and tibia length. These measurements were then utilized to calculate heart weight to body weight and heart weight to tibia length, both of which are used as an index for cardiac hypertrophy. Heart weight to body weight (HW/BW) was without significant changes in P209L mice compared with controls at 16 months of age (Figure 2C). The calculated heart weight to tibia length (HW/TL) ratios of the heterozygous and homozygous P209L knock-in mice were also comparable to the HW/TL ratio of the WT control littermates (Figure 2D).

To further characterize cardiac phenotypic changes due to the P209L mutation, we performed Hematoxylin and Eosin staining and Masson's trichrome staining to assess for the cardiac injury, morphological changes, and fibrosis. Morphological and histological analysis of BAG3-knock-in hearts did not reveal abnormal in cardiac morphology. Both homozygous and heterozygous mutant hearts did not exhibit any signs of cardiac hypertrophy or dilation. Furthermore, based on the Masson's Trichrome staining, there is no evidence of fibrosis in the P209L mutation mouse lines compared with the littermate control (Figure 2B).

Consistent with a lack of evidence providing physiological proof of cardiac remodeling, the qRT-PCR analysis of cardiac fetal gene markers there were no significant changes in levels of atrial natriuretic factor (ANF) and B-type natriuretic peptide (BNP), in the hearts of BAG3 P209L heterozygous (m/+) mice, BAG3 P209L homozygous (m/m) mice at 16 months of age (Figure 2E), compared with control littermates. Similarly, the expression levels of profibrotic genes collagen α1 types I (Col1a1) and III (Col3a1) (Figure 2F) are no difference compared with wild-type control.

To access the cardiac function in BAG3 P209 mutant mice, we performed cardiac physiological studies over the course of 16 months on P209L knock-in mice. Echocardiography revealed that left ventricular systolic function and left ventricular chamber morphology are grossly intact without abnormalities. The difference in percentage of fractional shortening [FS] at Week 18 and 47 for the three groups are statistically insignificant (Figure 3A). By week 66, the wild-type control, heterozygous, and homozygous P209L mutant mice samples all had nearly identical percentage of fractional shortening (FS), which indicates that the left ventricular (LV) systolic function are not affected by the P209L mutation.

As evidenced by the nearly identical end-diastolic LV internal diameter (LVIDd) and end-systolic LV internal diameter (LVIDs), there is no statistical difference in the LVIDd (Figure 3B) and LVIDs (Figure 3C) measurements among the wild-type and the two P209L mutant mice line. The end-diastolic left ventricular posterior wall thickness (LVPWd) of the heterozygous BAG3 P209L and homozygous BAG3 P209L mutant mouse hearts are within the normal limits and comparable with the control littermate. Consistent with histological observations, these

findings suggest that the missense P209L mutation did not result in left ventricular chamber dilation.

Effects of P209L Mutation on Expression Levels of Molecular Chaperones

To determine the effects of P209L missense mutation on expression levels of the chaperone complex, we evaluated protein samples from isolated cardiac tissue of 16-month-old BAG3 P209L heterozygous and homozygous knock-in mice and control mice. It has been previously shown BAG3 interacts with ATP-dependent high molecular weight chaperones such as HSP70 family with its BAG domain and interacts sHSPs through its 2 IPV motifs (32, 33, 35). Western blot analysis revealed that the levels of stress-inducible HSPs, such as HSP90 and HSP70, were without significant changes in P209L knock-in mouse cardiac tissues. The levels of the constitutively expressed HSC70 were also unchanged (Figure 2, A and B). Surprisingly, the protein levels of sHSPs, such as HSPB8 (also known as HSP22), HSPB6 (also known as HSP20), and HSPB5 (also known as αB-crystallin) did not undergo any obvious changes in P209L knock-in hearts. These data suggested that P209L mutation did not create increased protein stress in cardiac tissue.

Effects of P209L Mutation on Ubiquitination Degradative Pathway

It has been determined that BAG3 is involved with protein degradation via the ubiquitination pathway. To investigate whether the BAG3 P209L mutation leads to increased ubiquitinated proteins in cardiac tissue, Western blot analysis of ubiquitinated proteins was performed using anti-ubiquitin antibodies. Western blotting revealed no significant accumulation of ubiquitinated proteins in heterozygous BAG3 P209L-mutant (m/+), and homozygous BAG3 P209L-mutant (m/m) mouse hearts compared with wild-type mouse hearts (Figure 4D).

Effects of P209L Mutation on Autophagy

As it has been reported that BAG3 is involved in autophagy (37), our lab has previously shown that loss of BAG3 function suppresses autophagosome formation through examining the levels of the autophagosome-associated protein light chain 3B (LC3B) and selective autophagy receptor p62 (38). The formation of autophagosomes is the onset of a dynamic process known as autophagic flux that results in degradation of the formed autophagosome after fusion with lysosomes (42). Suppressed autophagic flux in BAG3-deficient hearts might lead to misfolded protein aggregates in cardiac myocytes (55). To investigate if the P209L mutation in the IPV motif affects the autophagic flux, Western blotting was performed, which showed no significant difference in the levels of LC3B and p62 levels in wild-type control, heterozygous, and homozygous P209L mutant mice heart tissues (Figure 4C). This suggests that the P209L mutation does not interfere with the level of autophagic flux.

DISCUSSION

BAG3 plays an integral role in the maintenance of normal cardiac function. An essential component of the protein quality control system in cardiomyocytes, BAG3 helps maintain protein homeostasis and cardiac function by exercising quality control over a specific subset of proteins required for metabolic and contractile function of cardiomyocytes (55). Mutations and downregulation of BAG3 have been reported to lead to cardiomyopathy and heart failure in numerous patient cases. Although it has been shown that BAG3 P209L mutant in human patients leads to development of dilated cardiomyopathy and progressive loss of cardiac function, little is known the pathogenesis of and molecular mechanism by BAG3 P209L missense mutation leads to progression of cardiomyopathy.

Our present study uses knock-in mice to elucidate the functional effects of the BAG3 P209L mutation in mice and investigate the molecular mechanism of P209L mutation in cardiomyopathy. We performed a comprehensive time course of cardiac physiological studies to assess long-term effects of P209L mutation on cardiac function in P209L knock-in mice, compared to littermate controls. No premature death of BAG3 P209L mice is observed. We did not observe any statistical difference in terms of survival rate for the three groups. Additionally, heart weight to body weight (HW/BW) and heart weight to tibia length (HW/TL) ratios were also assessed. There were no significant changes in P209L mice compared with controls. The expression levels of the cardiac fetal gene markers and profibrotic genes were within normal limits compared to that of the control mice. Furthermore, histological analysis revealed that mutant hearts did not exhibit any signs of cardiac hypertrophy, dilation or increased fibrosis. Together, our data suggest that the P209L mutation did not affect the survival of the mice or cause measurable cardiac hypertrophy and fibrosis.

Echocardiography of the mouse hearts shows that left ventricular systolic function was unaffected by the BAG3 P209L mutation. The end-diastolic left ventricular posterior wall thickness, end-diastolic LV internal diameter (LVIDd), and end-systolic LV internal diameter (LVIDs) of the mutant mice were comparable with the control. Consistent with histological observation, these observations suggest that P209L mutation does not lead to left ventricular chamber dilation or other pathological abnormalities of the heart.

BAG3 is implicated in ubiquitin degradation pathway and autophagy. To determine the role of P209L mutation in protein degradation and autophagy, we performed Western blot of ubiquitinated proteins in cardiac tissue and markers of autophagy. Western blot analysis revealed no significant changes in the level of ubiquitinated proteins or autophagosome proteins in the hearts, suggesting that BAG3 P209L mutation affect neither autophagy nor protein degradation through the ubiquitination pathway in cardiac tissues.

The ATP-dependent HSP70 and the ATP-independent small sHSP/HSPB family, which includes HSPB8, HSPB6, and HSPB5, constitute an ancient system for protecting proteins under conditions of proteotoxic stress (52). Small heat shock proteins lack the ATPase activity and must work in conjunction with HSP70 family to carry out active refolding of aberrant polypeptides. BAG3 can bind HSP70 with high affinity through its BAG domain BAG3, and BAG3 also interacts with sHSPs through its two IPV motifs (55). Therefore, BAG3 is functionally important for the chaperone complex function because of its ability to facilitate the assembly of large multi-chaperone complexes. Previous studies have shown that impaired interaction between BAG3 and HSP70 leads to degradation of sHSPs and increased

accumulation of protein substrates in the insoluble fractions (55). However, our western blot of BAG3-associated chaperones, such as HSC/HSP70 and sHSPs, such as HSPB5, HSPB6, HSPB8, in the 2 BAG3 P209L mutant mice and control mice. The Western blotting analysis revealed that there is no change in levels of BAG3-associated molecular chaperones such as the HSC/HSP70 as well as the sHSPs in the P209L mutant mice hearts compared with the control mice. Our present observations suggested that this residue does not cause loss of function of BAG3 and is not critical for the essential function of BAG3 in mice. However, our present study does not provide insight into the potential changes or disruption of the interaction between BAG3 and its associated molecular chaperones. In future experiments, the immunoprecipitation analysis and co-localization immunofluorescence analysis would be performed on protein extracts from BAG3 P209L and control mice to directly assess potential changes in the physical interactions between components of the BAG3-multi-chaperone complex. To study the effect of P209L on the interaction affinity between BAG3 and sHSPs, we also will perform isothermal titration calorimetry (ITC) experiment to measure the BAG3 P209L mutant and HSPB8 interaction affinity.

The P209L mutation is the unequivocal cause of cardiomyopathy and progressive loss of cardiac function in human. In addition, the Proline 209 residue and adjacent region are 100% conserved between human and mouse (60). Our observation of no baseline cardiac phenotype in BAG3 P209L knock-in mice was quite unexpected. There are several possible interpretations of this observation, one of which is that it may take a considerable amount of time to develop severe cardiomyopathy due to aberrant protein aggregation. We only evaluated cardiac structure and function of BAG3 P209L knock-in mice, which were in a pure C57/B6 genetic background,

at baseline conditions up to 16 months of age. Future studies are needed to determine whether BAG3 P209L knock-in mice would eventually develop cardiomyopathy with greater age and to determine whether BAG3 P209L knock-in mice respond normally to cardiac stress, such as TAC-induced pressure overload. The other potential explanation is that the P209L mutation may not totally diminish the binding affinity of the IPV motif for sHSPs or lead to degradation of sHSPs. There are two IVP motifs in BAG3, both of which are capable of interaction with sHSPs. Through studying the structure of BAG3, we learned that the P209L mutation is located in one of the two IPV motifs. Perhaps, the P209L mutation does indeed cause impaired interaction between BAG3 and sHSPs, but the second IVP motif in mice is able to compensate for the loss of function at the first IPV motif. We are currently generating a novel knock-in mouse model carries Proline to Leucine mutations in both IPV motifs, which will be used to elucidate the function of two IPV motifs in BAG3 in vivo. Lastly, an unknown genetic modifier could be required to manifest a cardiomyopathy phenotype, which can be further validated by studying BAG3 P209L mutant mice in different inbred mouse strains.

FIGURES

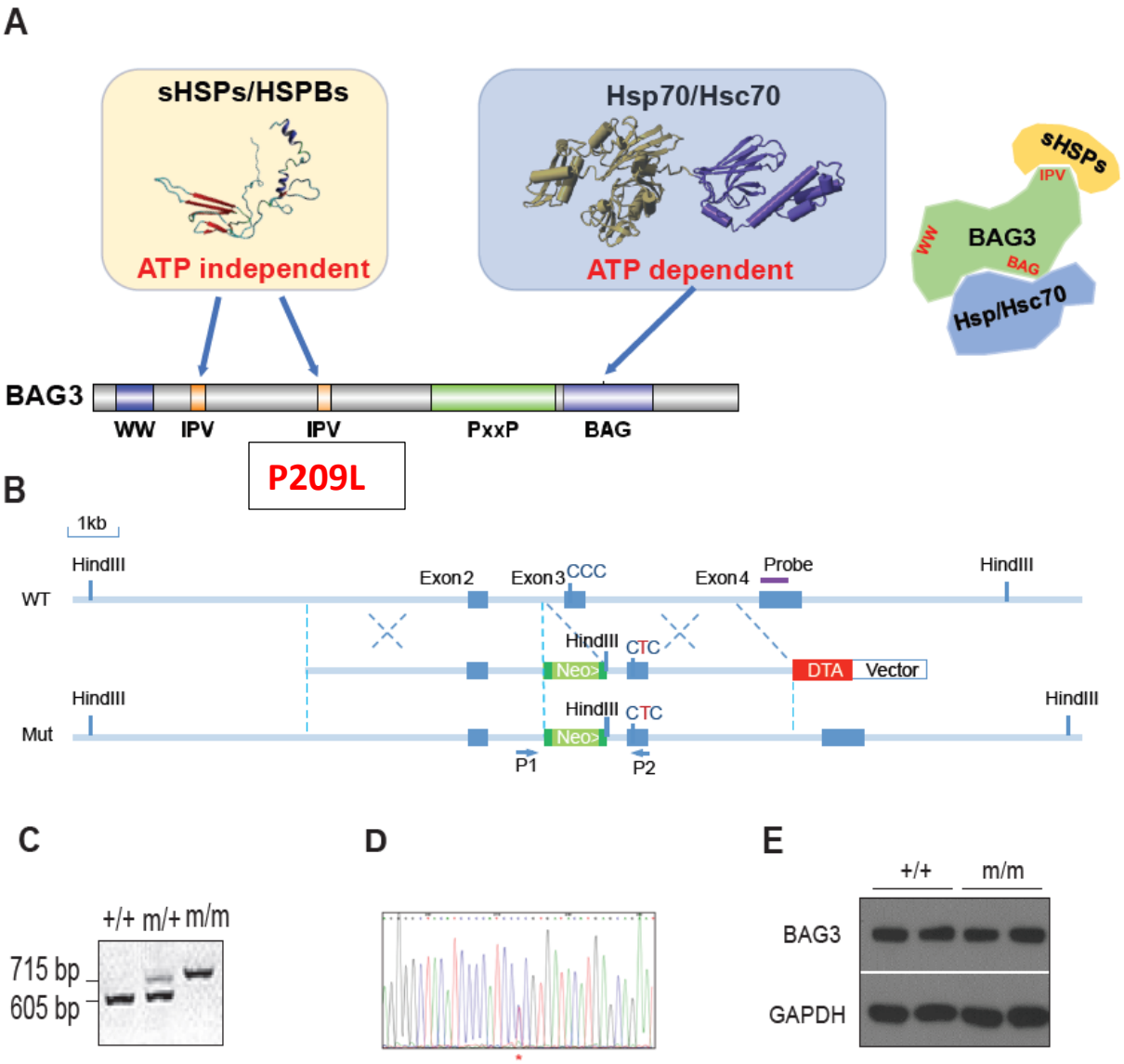

Figure 1. **Generation of heterozygous BAG3 P209L-mutant (m/+) and homozygous BAG3 P209L-mutant (m/m) mice.** (A) Protein binding domains of BAG3. (B) Construct of P209L mutation. (C) Genotyping of result the mutant mice (D) Sequence result confirms the mutation. (E) Western blot analysis of BAG3 protein levels in control mice and homozygous BAG3 P209L mutant mice at 4 months of age.

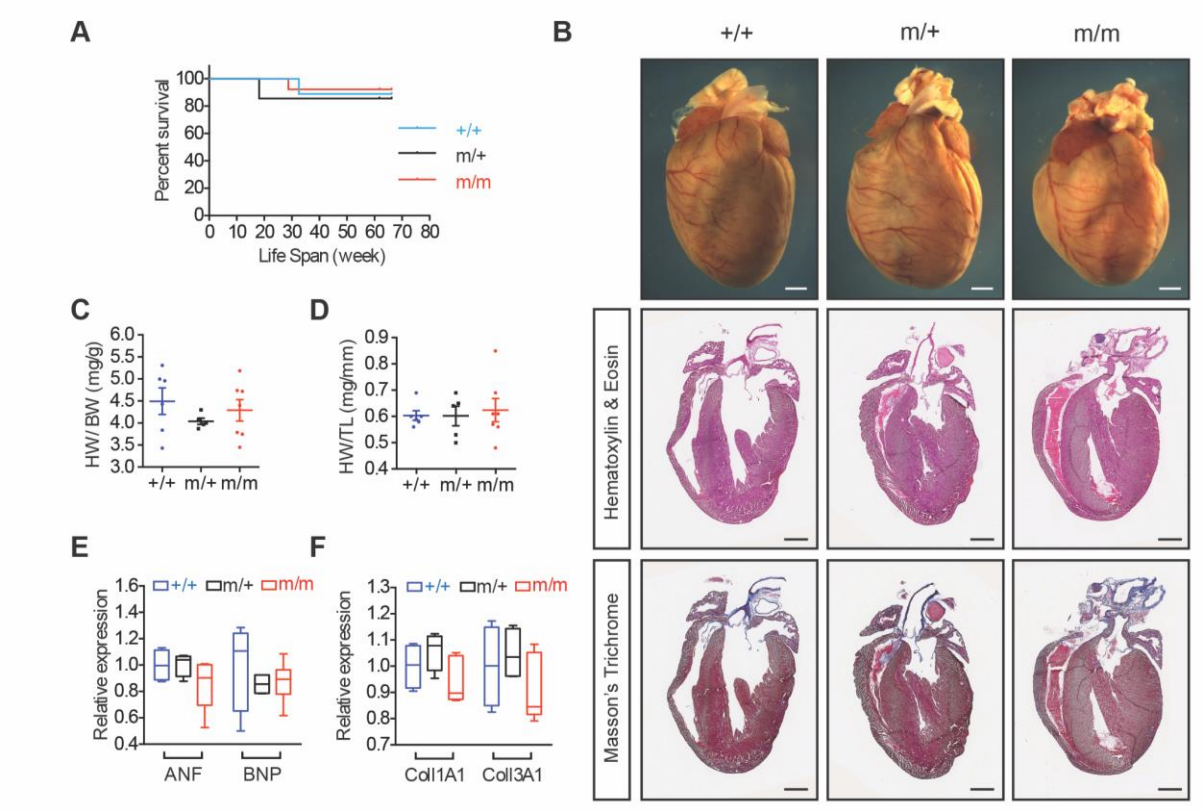

Figure 2. **P209L in BAG3 did not lead to cardiac dilation, fibrotic changes or premature death.** (**A**)Kaplan-Meier survival curves for homozygous P209L mutant mice (n = 9), heterozygous P209L mutant mice (n = 8), and control (n = 9) mice. (**B**) Representative microscopic views of whole mouse hearts (top, scale bars: 1 mm) and cross-sectional views of H&E-stained (middle, scale bars: 1 mm) and Masson's trichrome–stained (bottom, scale bars: 50 μm) hearts isolated from control, heterozygous P209L mice, and homozygous P209L mice at 16 months of age. (**C-D**) HW to BW ratio (**C**) and HW to TL ratio (**D**) for control (n = 5) versus heterozygous P209L mice (n = 5) and homozygous P209L mice (n = 7) mice at 16 months of age. (**E-F**) qRT-PCR analysis of cardiac fetal gene markers (**E**) and profibrotic genes (**F)** in control (n = 5), heterozygous P209L mice (n = 5), and homozygous P209L mice (n = 7) mouse hearts at 16 months of age.

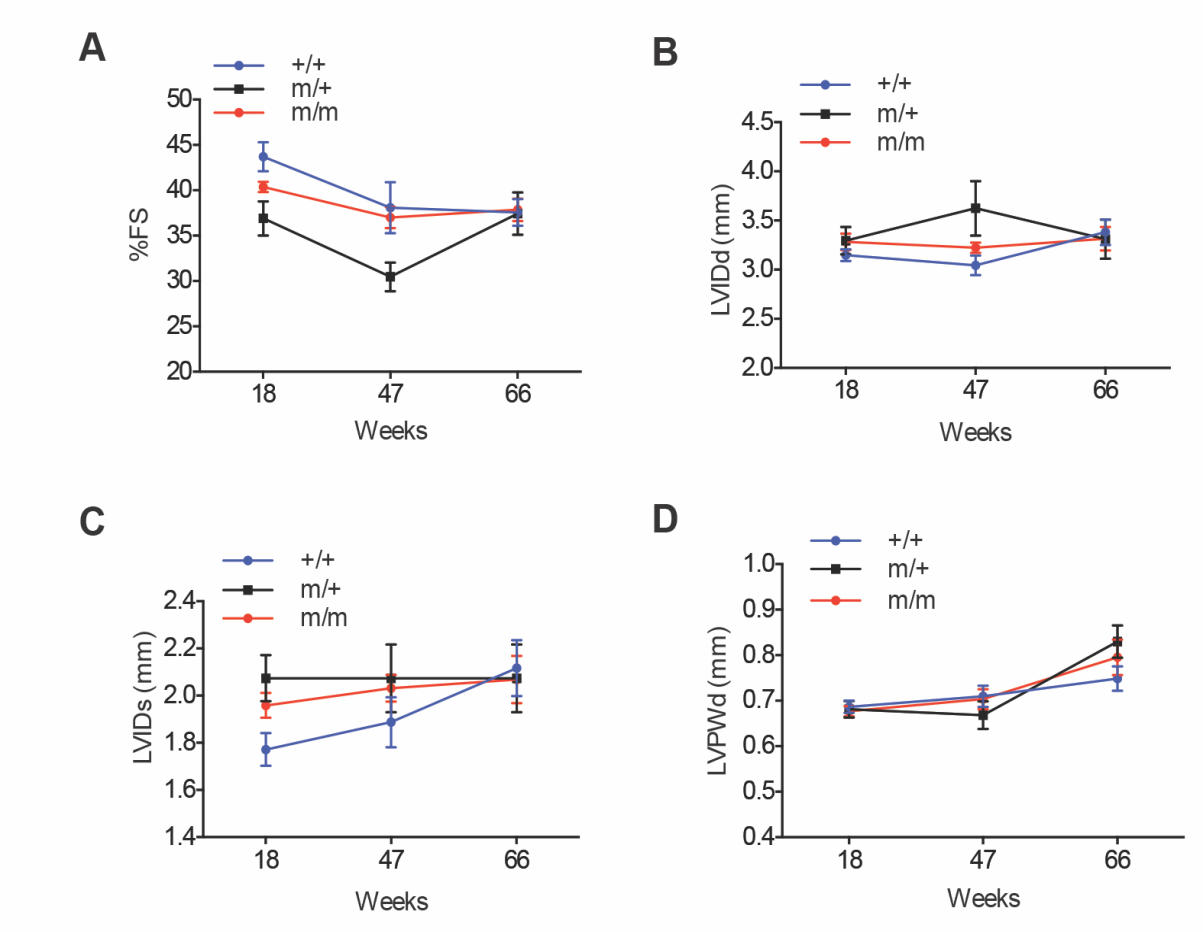

Figure 3. **Echocardiography shows normal systolic function with no evidence left ventricular dilation in the heterozygous and homozygous P209L mutant mice compared with control littermates.** (**A–D**) Echocardiographic measurements for control, heterozygous P209L mice, and homozygous P209L mice (n = 8 -10 mice at 18, 47, and 66 weeks of age) of (**A**) left ventricular percentage of fractional shortening (% FS), (**B**) end-diastolic LV internal diameter (LVIDd), (**C**) end systolic left ventricular internal diameter (LVIDs), and (**D**) end-diastolic left ventricular posterior wall thickness (LVPWd).

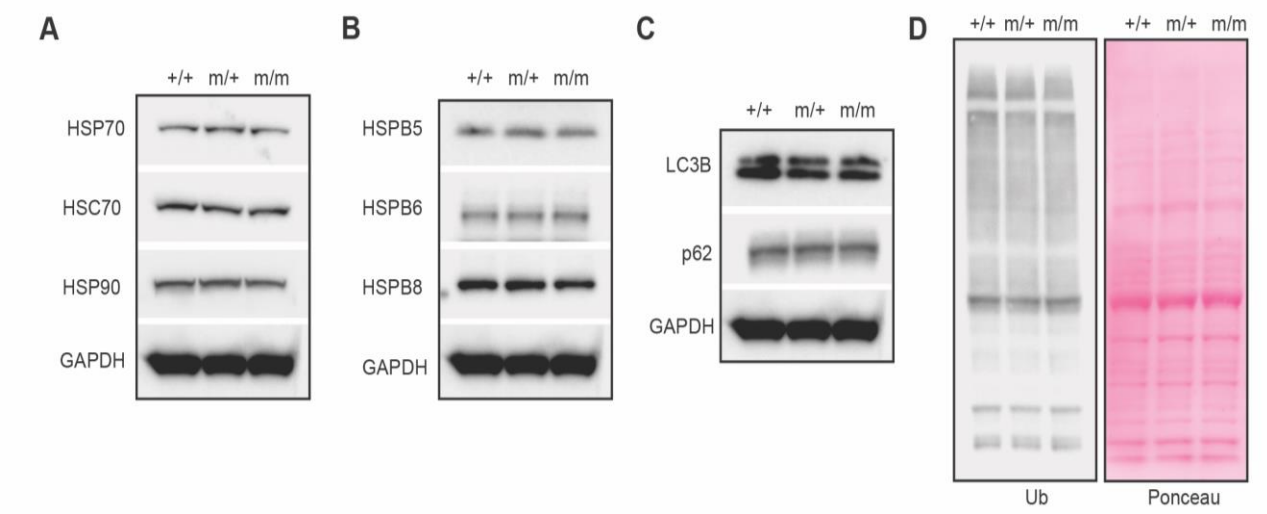

Figure 4. **P209L mutation in the IPV motif of BAG3 does not affect the protein levels of heat shock proteins.** (**A**) Representative Immunoblots of HSP90, HSP70, and HSC70 in WT (+/+), heterozygous BAG3 P209L-mutant (m/+), and homozygous BAG3 P209L-mutant (m/m) mouse hearts. Representative Western blot (**B**) of HSPB5, HSPB6, and HSPB8 in WT (+/+), heterozygous BAG3 P209L-mutant (m/+), and homozygous BAG3 P209L-mutant (m/m) mouse hearts. GAPDH served as a loading control (n = 3 mice per group). **(C)** Western blot analysis of LC3B and p62 levels in wild-type control (+/+), heterozygous BAG3 P209L-mutant (m/+), and homozygous BAG3 P209L-mutant (m/m) mouse hearts. (n = 3 mice per group). **(D)** Western blot analysis of ubiquitinated proteins in WT (+/+), heterozygous BAG3 P209L-mutant (m/+), and homozygous BAG3 P209L-mutant (m/m) mouse hearts. The samples were probed with anti-ubiquitin antibodies. Ponceau staining image indicates consistency in sample loading. (n = 3 mice per group).

TABLES

Table 1. Antibody List

Antibody	**Source, Cat. No**
GAPDH	Santa cruz, sc-32233
BAG3	Proteintech, 10599-1-AP
LC3B	Cell Signaling, 2775S
SQSTM1/p62	PROGEN Biotechnik, GP62-C
HSP90	Abcam, ab178854
HSP20/HSPB6	R&D, MAB4200
HSP22/ HSPB8	Abcam ab151552 or provide by Hongyu Qiu(11)
αB-crystallin/ HSPB5	Enzo Life Sciences, ADISPA-223
HSP70/HSP72	Enzo Life Sciences, ADISPA-810-D
HSC70/HSP73	Enzo Life Sciences, ADISPA-815-F

Table 2. Primer List

Gene	**Forward**	**Reverse**
ANF	GATAGATGAAGGCAGGAAGCCGC	AGGATTGGAGCCCAGAGTGGACTA
BNP	TGTTTCTGCTTTTCCTTTATCTGTC	CTCCGACTTTTCTCTTATCAGCTC
Collagen 1a1	TCACCAAACTCAGAAGATGTAGGA	GACCAGGAGGACCAGGAAG
Collagen 3a1	ACAGCAGTCCAACGTAGATGAAT	TCACAGATTATGTCATCGCAAAG

REFERENCES

1. Wang X, Robbins J. Heart failure and protein quality control. Circulation research. 2006;99(12):1315-28. doi: 10.1161/01.RES.0000252342.61447.a2. PubMed PMID: 17158347.

2. Broadley SA, Hartl FU. The role of molecular chaperones in human misfolding diseases. FEBS letters. 2009;583(16):2647-53. doi: 10.1016/j.febslet.2009.04.029. PubMed PMID: 19393652.

3. Frydman J. Folding of newly translated proteins in vivo: the role of molecular chaperones. Annual review of biochemistry. 2001;70:603-47. doi: 10.1146/annurev.biochem.70.1.603. PubMed PMID: 11395418.

4. Young JC, Agashe VR, Siegers K, Hartl FU. Pathways of chaperone-mediated protein folding in the cytosol. Nature reviews Molecular cell biology. 2004;5(10):781-91. doi: 10.1038/nrm1492. PubMed PMID: 15459659.

5. Arimura T, Ishikawa T, Nunoda S, Kawai S, Kimura A. Dilated cardiomyopathy-associated BAG3 mutations impair Z-disc assembly and enhance sensitivity to apoptosis in cardiomyocytes. Human mutation. 2011;32(12):1481-91. doi: 10.1002/humu.21603. PubMed PMID: 21898660.

6. Chami N, Tadros R, Lemarbre F, Lo KS, Beaudoin M, Robb L, Labuda D, Tardif JC, Racine N, Talajic M, Lettre G. Nonsense Mutations in BAG3 are Associated With Early-Onset Dilated Cardiomyopathy in French Canadians. The Canadian journal of cardiology. 2014;30(12):1655-61. doi: 10.1016/j.cjca.2014.09.030. PubMed PMID: 25448463.

7. Feldman AM, Begay RL, Knezevic T, Myers VD, Slavov DB, Zhu W, Gowan K, Graw SL, Jones KL, Tilley DG, Coleman RC, Walinsky P, Cheung JY, Mestroni L, Khalili K, Taylor MR. Decreased levels of BAG3 in a family with a rare variant and in idiopathic dilated cardiomyopathy. Journal of cellular physiology. 2014;229(11):1697-702. doi: 10.1002/jcp.24615. PubMed PMID: 24623017.

8. Norton N, Li D, Rieder MJ, Siegfried JD, Rampersaud E, Zuchner S, Mangos S, Gonzalez-Quintana J, Wang L, McGee S, Reiser J, Martin E, Nickerson DA, Hershberger RE. Genome-wide studies of copy number variation and exome sequencing identify rare variants in BAG3 as a cause of dilated cardiomyopathy. American journal of human genetics. 2011;88(3):273-82. doi: 10.1016/j.ajhg.2011.01.016. PubMed PMID: 21353195; PubMed Central PMCID: PMC3059419.

9. Selcen D, Muntoni F, Burton BK, Pegoraro E, Sewry C, Bite AV, Engel AG. Mutation in BAG3 causes severe dominant childhood muscular dystrophy. Annals of neurology. 2009;65(1):83-9. doi: 10.1002/ana.21553. PubMed PMID: 19085932; PubMed Central PMCID: PMC2639628.

10. Villard E, Perret C, Gary F, Proust C, Dilanian G, Hengstenberg C, Ruppert V, Arbustini E, Wichter T, Germain M, Dubourg O, Tavazzi L, Aumont MC, DeGroote P, Fauchier L, Trochu JN, Gibelin P, Aupetit JF, Stark K, Erdmann J, Hetzer R, Roberts AM, Barton PJ, Regitz-Zagrosek V, Cardiogenics C, Aslam U, Duboscq-Bidot L, Meyborg M, Maisch B, Madeira H, Waldenstrom A, Galve E, Cleland JG, Dorent R, Roizes G, Zeller T, Blankenberg S, Goodall AH, Cook S, Tregouet DA, Tiret L, Isnard R, Komajda M, Charron P, Cambien F. A genome-wide association study identifies two loci associated with heart failure due to dilated cardiomyopathy. European heart journal. 2011;32(9):1065-76. doi: 10.1093/eurheartj/ehr105. PubMed PMID: 21459883; PubMed Central PMCID: PMC3086901.

11. Takayama S, Xie Z, Reed JC. An evolutionarily conserved family of Hsp70/Hsc70 molecular chaperone regulators. The Journal of biological chemistry. 1999;274(2):781-6. PubMed PMID: 9873016.

12. Rosati A, Graziano V, De Laurenzi V, Pascale M, Turco MC. BAG3: a multifaceted protein that regulates major cell pathways. Cell death & disease. 2011;2:e141. doi: 10.1038/cddis.2011.24. PubMed PMID: 21472004; PubMed Central PMCID: PMC3122056.

13. Takayama S, Reed JC. Molecular chaperone targeting and regulation by BAG family proteins. Nature cell biology. 2001;3(10):E237-41. doi: 10.1038/ncb1001-e237. PubMed PMID: 11584289.

14. Doong H, Vrailas A, Kohn EC. What's in the 'BAG'?--A functional domain analysis of the BAG-family proteins. Cancer letters. 2002;188(1-2):25-32. PubMed PMID: 12406544.

15. Carra S, Seguin SJ, Lambert H, Landry J. HspB8 chaperone activity toward poly(Q)-containing proteins depends on its association with Bag3, a stimulator of macroautophagy. The Journal of biological chemistry. 2008;283(3):1437-44. doi: 10.1074/jbc.M706304200. PubMed PMID: 18006506.

16. Fuchs M, Poirier DJ, Seguin SJ, Lambert H, Carra S, Charette SJ, Landry J. Identification of the key structural motifs involved in HspB8/HspB6-Bag3 interaction. The Biochemical journal. 2010;425(1):245-55. doi: 10.1042/BJ20090907. PubMed PMID: 19845507.

17. Carra S. The stress-inducible HspB8-Bag3 complex induces the eIF2alpha kinase pathway: implications for protein quality control and viral factory degradation? Autophagy. 2009;5(3):428-9. PubMed PMID: 19202352.

18. Gamerdinger M, Hajieva P, Kaya AM, Wolfrum U, Hartl FU, Behl C. Protein quality control during aging involves recruitment of the macroautophagy pathway by BAG3. The EMBO journal. 2009;28(7):889-901. doi: 10.1038/emboj.2009.29. PubMed PMID: 19229298; PubMed Central PMCID: PMC2647772.

19. Gamerdinger M, Carra S, Behl C. Emerging roles of molecular chaperones and co-chaperones in selective autophagy: focus on BAG proteins. Journal of molecular medicine. 2011;89(12):1175-82. doi: 10.1007/s00109-011-0795-6. PubMed PMID: 21818581.

20. Behl C. BAG3 and friends: co-chaperones in selective autophagy during aging and disease. Autophagy. 2011;7(7):795-8. doi: 10.4161/auto.7.7.15844. PubMed PMID: 21681022.

21. Chen Y, Yang LN, Cheng L, Tu S, Guo SJ, Le HY, Xiong Q, Mo R, Li CY, Jeong JS, Jiang L, Blackshaw S, Bi LJ, Zhu H, Tao SC, Ge F. Bcl2-associated athanogene 3 interactome analysis reveals a new role in modulating proteasome activity. Molecular & cellular proteomics : MCP. 2013;12(10):2804-19. doi: 10.1074/mcp.M112.025882. PubMed PMID: 23824909; PubMed Central PMCID: PMC3790292.

22. Homma S, Iwasaki M, Shelton GD, Engvall E, Reed JC, Takayama S. BAG3 deficiency results in fulminant myopathy and early lethality. The American journal of pathology. 2006;169(3):761-73. doi: 10.2353/ajpath.2006.060250. PubMed PMID: 16936253; PubMed Central PMCID: PMC1698816.

23. Youn DY, Lee DH, Lim MH, Yoon JS, Lim JH, Jung SE, Yeum CE, Park CW, Youn HJ, Lee JS, Lee SB, Ikawa M, Okabe M, Tsujimoto Y, Lee JH. Bis deficiency results in early lethality with metabolic deterioration and involution of spleen and thymus. American journal of physiology Endocrinology and metabolism. 2008;295(6):E1349-57. doi: 10.1152/ajpendo.90704.2008. PubMed PMID: 18840758.

24. Balch WE, Morimoto RI, Dillin A, Kelly JW. Adapting proteostasis for disease intervention. Science. 2008;319(5865):916-9. doi: 10.1126/science.1141448. PubMed PMID: 18276881.

25. Hartl FU, Bracher A, Hayer-Hartl M. Molecular chaperones in protein folding and proteostasis. Nature. 2011;475(7356):324-32. doi: 10.1038/nature10317. PubMed PMID: 21776078.

26. Lee S, Tsai FT. Molecular chaperones in protein quality control. Journal of biochemistry and molecular biology. 2005;38(3):259-65. PubMed PMID: 15943899.

27. Marian AJ. Modeling human disease phenotype in model organisms: "It's only a model!". Circulation research. 2011;109(4):356-9. doi: 10.1161/CIRCRESAHA.111.249409. PubMed PMID: 21817163; PubMed Central PMCID: PMC3160674.

28. Ulbricht A, Arndt V, Hohfeld J. Chaperone-assisted proteostasis is essential for mechanotransduction in mammalian cells. Communicative & integrative biology. 2013;6(4):e24925. doi: 10.4161/cib.24925. PubMed PMID: 23986815; PubMed Central PMCID: PMC3737759.

29. Hartl FU, Hayer-Hartl M. Molecular chaperones in the cytosol: from nascent chain to folded protein. Science. 2002;295(5561):1852-8. doi: 10.1126/science.1068408. PubMed PMID: 11884745.

30. Kettern N, Dreiseidler M, Tawo R, Hohfeld J. Chaperone-assisted degradation: multiple paths to destruction. Biological chemistry. 2010;391(5):481-9. doi: 10.1515/BC.2010.058. PubMed PMID: 20302520.

31. Breusing N, Grune T. Regulation of proteasome-mediated protein degradation during oxidative stress and aging. Biological chemistry. 2008;389(3):203-9. doi: 10.1515/BC.2008.029. PubMed PMID: 18208355.

32. Nandi D, Tahiliani P, Kumar A, Chandu D. The ubiquitin-proteasome system. Journal of biosciences. 2006;31(1):137-55. PubMed PMID: 16595883.

33. Arndt V, Rogon C, Hohfeld J. To be, or not to be--molecular chaperones in protein degradation. Cellular and molecular life sciences : CMLS. 2007;64(19-20):2525-41. doi: 10.1007/s00018-007-7188-6. PubMed PMID: 17565442.

34. Massey AC, Zhang C, Cuervo AM. Chaperone-mediated autophagy in aging and disease. Current topics in developmental biology. 2006;73:205-35. doi: 10.1016/S0070-2153(05)73007-6. PubMed PMID: 16782460.

35. Arndt V, Dick N, Tawo R, Dreiseidler M, Wenzel D, Hesse M, Furst DO, Saftig P, Saint R, Fleischmann BK, Hoch M, Hohfeld J. Chaperone-assisted selective autophagy is essential for muscle maintenance. Current biology : CB. 2010;20(2):143-8. doi: 10.1016/j.cub.2009.11.022. PubMed PMID: 20060297.

36. Ulbricht A, Eppler FJ, Tapia VE, van der Ven PF, Hampe N, Hersch N, Vakeel P, Stadel D, Haas A, Saftig P, Behrends C, Furst DO, Volkmer R, Hoffmann B, Kolanus W, Hohfeld J. Cellular mechanotransduction relies on tension-induced and chaperone-assisted autophagy. Current biology : CB. 2013;23(5):430-5. doi: 10.1016/j.cub.2013.01.064. PubMed PMID: 23434281.

37. Arias E, Cuervo AM. Chaperone-mediated autophagy in protein quality control. Current opinion in cell biology. 2011;23(2):184-9. doi: 10.1016/j.ceb.2010.10.009. PubMed PMID: 21094035; PubMed Central PMCID: PMC3078170.

38. Cuervo AM. Autophagy: many paths to the same end. Molecular and cellular biochemistry. 2004;263(1-2):55-72. PubMed PMID: 15524167.

39. Lanneau D, Wettstein G, Bonniaud P, Garrido C. Heat shock proteins: cell protection through protein triage. TheScientificWorldJournal. 2010;10:1543-52. doi: 10.1100/tsw.2010.152. PubMed PMID: 20694452.

40. Mayer MP. Hsp70 chaperone dynamics and molecular mechanism. Trends in biochemical sciences. 2013;38(10):507-14. doi: 10.1016/j.tibs.2013.08.001. PubMed PMID: 24012426.

41. Mayer MP, Bukau B. Hsp70 chaperones: cellular functions and molecular mechanism. Cellular and molecular life sciences : CMLS. 2005;62(6):670-84. doi: 10.1007/s00018-004-4464-6. PubMed PMID: 15770419; PubMed Central PMCID: PMC2773841.

42. Bukau B, Horwich AL. The Hsp70 and Hsp60 chaperone machines. Cell. 1998;92(3):351-66. PubMed PMID: 9476895.

43. Zhuravleva A, Clerico EM, Gierasch LM. An interdomain energetic tug-of-war creates the allosterically active state in Hsp70 molecular chaperones. Cell. 2012;151(6):1296-307. doi: 10.1016/j.cell.2012.11.002. PubMed PMID: 23217711; PubMed Central PMCID: PMC3521165.

44. Zuiderweg ER, Bertelsen EB, Rousaki A, Mayer MP, Gestwicki JE, Ahmad A. Allostery in the Hsp70 chaperone proteins. Topics in current chemistry. 2013;328:99-153. doi: 10.1007/128_2012_323. PubMed PMID: 22576356; PubMed Central PMCID: PMC3623542.

45. Rudiger S, Germeroth L, Schneider-Mergener J, Bukau B. Substrate specificity of the DnaK chaperone determined by screening cellulose-bound peptide libraries. The EMBO journal. 1997;16(7):1501-7. doi: 10.1093/emboj/16.7.1501. PubMed PMID: 9130695; PubMed Central PMCID: PMC1169754.

46. Schlecht R, Erbse AH, Bukau B, Mayer MP. Mechanics of Hsp70 chaperones enables differential interaction with client proteins. Nature structural & molecular biology. 2011;18(3):345-51. doi: 10.1038/nsmb.2006. PubMed PMID: 21278757.

47. Shiber A, Ravid T. Chaperoning proteins for destruction: diverse roles of Hsp70 chaperones and their co-chaperones in targeting misfolded proteins to the proteasome. Biomolecules. 2014;4(3):704-24. doi: 10.3390/biom4030704. PubMed PMID: 25036888; PubMed Central PMCID: PMC4192669.

48. Stricher F, Macri C, Ruff M, Muller S. HSPA8/HSC70 chaperone protein: structure, function, and chemical targeting. Autophagy. 2013;9(12):1937-54. doi: 10.4161/auto.26448. PubMed PMID: 24121476.

49. Rauch JN, Gestwicki JE. Binding of human nucleotide exchange factors to heat shock protein 70 (Hsp70) generates functionally distinct complexes in vitro. The Journal of biological chemistry. 2014;289(3):1402-14. doi: 10.1074/jbc.M113.521997. PubMed PMID: 24318877; PubMed Central PMCID: PMC3894324.

50. Glembotski CC. The role of the unfolded protein response in the heart. Journal of molecular and cellular cardiology. 2008;44(3):453-9. doi: 10.1016/j.yjmcc.2007.10.017. PubMed PMID: 18054039; PubMed Central PMCID: PMC2746718.

51. Kabbage M, Dickman MB. The BAG proteins: a ubiquitous family of chaperone regulators. Cellular and molecular life sciences : CMLS. 2008;65(9):1390-402. doi: 10.1007/s00018-008-7535-2. PubMed PMID: 18264803.

52. Cheng H, Kimura K, Peter AK, Cui L, Ouyang K, Shen T, Liu Y, Gu Y, Dalton ND, Evans SM, Knowlton KU, Peterson KL, Chen J. Loss of enigma homolog protein results in dilated cardiomyopathy. Circulation research. 2010;107(3):348-56. doi: 10.1161/CIRCRESAHA.110.218735. PubMed PMID: 20538684; PubMed Central PMCID: PMC3684396.

53. Elengoe, Asita, Mohammed Abu Naser, and Salehhuddin Hamdan. "A Novel Protein Interaction between Nucleotide Binding Domain of Hsp70 and P53 Motif." International Journal of Genomics2015 (2015): 1-6. doi:10.1155/2015/391293.

54. Abel ED, Kaulbach HC, Tian R, Hopkins JC, Duffy J, Doetschman T, Minnemann T, Boers ME, Hadro E, Oberste-Berghaus C, Quist W, Lowell BB, Ingwall JS, Kahn BB. Cardiac hypertrophy with preserved contractile function after selective deletion of GLUT4 from the heart. The Journal of clinical investigation. 1999;104(12):1703-14. doi: 10.1172/JCI7605. PubMed PMID: 10606624; PubMed Central PMCID: PMC409881.

54. Assimon, V. A., Gillies, A. T., Rauch, J. N., & Gestwicki, J. E. (2012). Hsp70 Protein Complexes as Drug Targets. Current Pharmaceutical Design,19(3), 404-417. doi:10.2174/1381612811306030404

55. Fang, Xi, Julius Bogomolovas, Tongbin Wu, Wei Zhang, Canzhao Liu, Jennifer Veevers, Matthew J. Stroud, Zhiyuan Zhang, Xiaolong Ma, Yongxin Mu, Dieu-Hung Lao, Nancy D. Dalton, Yusu Gu, Celine Wang, Michael Wang, Yan Liang, Stephan Lange, Kunfu Ouyang, Kirk L. Peterson, Sylvia M. Evans, and Ju Chen. "Loss-of-function Mutations in Co-chaperone BAG3 Destabilize Small HSPs and Cause Cardiomyopathy." Journal of Clinical Investigation127, no. 8 (2017): 3189-200. doi:10.1172/jci94310.

56. Stürner, Elisabeth, and Christian Behl. “The Role of the Multifunctional BAG3 Protein in Cellular Protein Quality Control and in Disease.” Frontiers in Molecular Neuroscience, vol. 10, 2017, doi:10.3389/fnmol.2017.00177.

57. Merabova, N., Sariyer, I. K., Saribas, A. S., Knezevic, T., Gordon, J., Turco, M. C., . . . Khalili, K. (2014). WW Domain of BAG3 Is Required for the Induction of Autophagy in Glioma Cells. Journal of Cellular Physiology,230(4), 831-841. doi:10.1002/jcp.24811

58. Selcen, D., F. Muntoni, B. K. Burton, E. Pegoraro, C. Sewry, A. V. Bite, and A. G. Engel. "Mutation in BAG3 Causes Severe Dominant Childhood Muscular Dystrophy." Annals of Neurology. January 2009. Accessed May 29, 2018. https://www.ncbi.nlm.nih.gov/pubmed/19085932.

59. Quintana, M. T., Parry, T. L., He, J., Yates, C. C., Sidorova, T. N., Murray, K. T., . . . Willis, M. S. (2016). Cardiomyocyte-Specific Human Bcl2-Associated Anthanogene 3 P209L Expression Induces Mitochondrial Fragmentation, Bcl2-Associated Anthanogene 3 Haploinsufficiency, and Activates p38 Signaling. The American Journal of Pathology,186(8), 1989-2007. doi:10.1016/j.ajpath.2016.03.017

60. Zhang, Zhiwei, Matthew J. Stroud, Jianlin Zhang, Xi Fang, Kunfu Ouyang, Kensuke Kimura, Yongxin Mu, Nancy D. Dalton, Yusu Gu, William H. Bradford, Kirk L. Peterson, Hongqiang Cheng, Xinmin Zhou, and Ju Chen. "Normalization of Naxos Plakoglobin Levels Restores Cardiac Function in Mice." Journal of Clinical Investigation125, no. 4 (2015): 1708-712. doi:10.1172/jci80335.